CHAPTER IV
RESULTS AND DISCUSSION

4.1 Inclusion compound of CA-VCM

VCM has the low boiling point (-13.4°C) and is volatile at room temperature, thus, the preparation of inclusion compound can not be achieved by the ordinary recrystallization procedure. CA is an attractive host compound owing to the inclusion compound formation by guest absorption into guest free crystal. Miyata *et al.* (1990) reported that inclusion compound of CA-guest responds another guest by changing its packing structure. Thus, it is expected that CA provides the channel for guest after the adsorption or insertion was proceeded. Tsutsumi *et al.* (1990) clarified the successful inclusion polymerization of 1-chlorobutadiene by using guest adsorption on the guest free crystal of deoxycholic acid and found that poly(1-chlorobutadiene) has almost 100% of head to tail, trans-1,4-structure on the basic of ^{13}C-NMR and also optically active was obtained.

In the present work, in order to obtain the CA-guest free crystal, methylmethacrylate (MMA) was chosen as a guest to prepare CA-MMA in the first step, followed by the guest exclusion by heating CA-MMA under vacuo for overnight. The crystal structure of CA-MMA is a monoclinic (P2$_1$) with MMA aligned in each CA phase. Considering the size of MMA molecule, it can be expected that the channel remained after MMA exclusion be appropriate for VCM.

VCM adsorption into guest free CA was studied by FTIR. As shown in Figure 4.1(a), the successful CA-MMA inclusion compound is confirmed as referred to the peaks 1 699 cm^{-1} for carbonyl group and 1 633 cm^{-1} for C=C stretching of MMA, and 1 720 cm^{-1} for carbonyl group of CA. After guest exclusion process, the FTIR turns to the pattern of CA with a significant peak 1 720 cm^{-1} (Figure 4.1(b)). After the guest free CA was immersed in

liquidified VCM under −15 °C, the peaks 1 604 cm^{-1} for C=C stretching, and 3 084 cm^{-1} for C-H stretching of VCM, are observed (Figure 4.1(c)). This implied that the VCM adsorption into the CA channel was successful.

The VCM adsorption into CA channel was also studied by low temperature DSC. The analysis of the CA-VCM adduct was carried out from -20° to 200°C to define the thermal stability of CA after VCM adsorption. After VCM adsorption, CA shows endothermic broad peak in the range of 40°-50°C (Figure 4.2b) as compared to the CA before VCM adsorption (Figure 4.2a). This implied that VCM is a guest inserted in CA channel. It should be noted that the release temperature of VCM is much higher than VCM boiling point for over 50°C. Thermogravimetry analysis by TGA (Figure 4.3) indicates that the VCM guest is released out from CA channel starting from 40°C to nearly 60°C with the weight loss 11.75%, indicating that a host-guest ratio 1:1.

X-ray diffraction pattern is an alternative way to confirm CA-VCM adduct. It can be expected that after the inclusion occurred, the crystal pattern would change.

The XRD pattern of CA guest free (Figure 4.4(a)) shows 2θ at 7.46, 10.4, 11.8, 12.9, and 14.9°, which can be referred to crystal structure of orthorhombic (p2$_1$2$_1$2$_1$), as reported by Miyata $et\ al.$ (1990). After immersing in liquidified VCM under −15°C for 2-7 days, the XRD pattern was changed gradually. As shown in Figure 4.4(c), after VCM adsorption proceeded for 2 days, the XRD pattern showed the peaks different from that of the CA. However, when the guest adsorption time was passed for more than 2 days, the XRD pattern was totally different (Figure 4.4(b)) with significant 2θ peaks at 7.3, 8.2, 11.3, 12.9, 14.0, 15.0, 16.6, and 18.3. This implied that VCM was included inside CA-guest free channel by guest adsorption and stabilized as a result of CA packing structure changing.
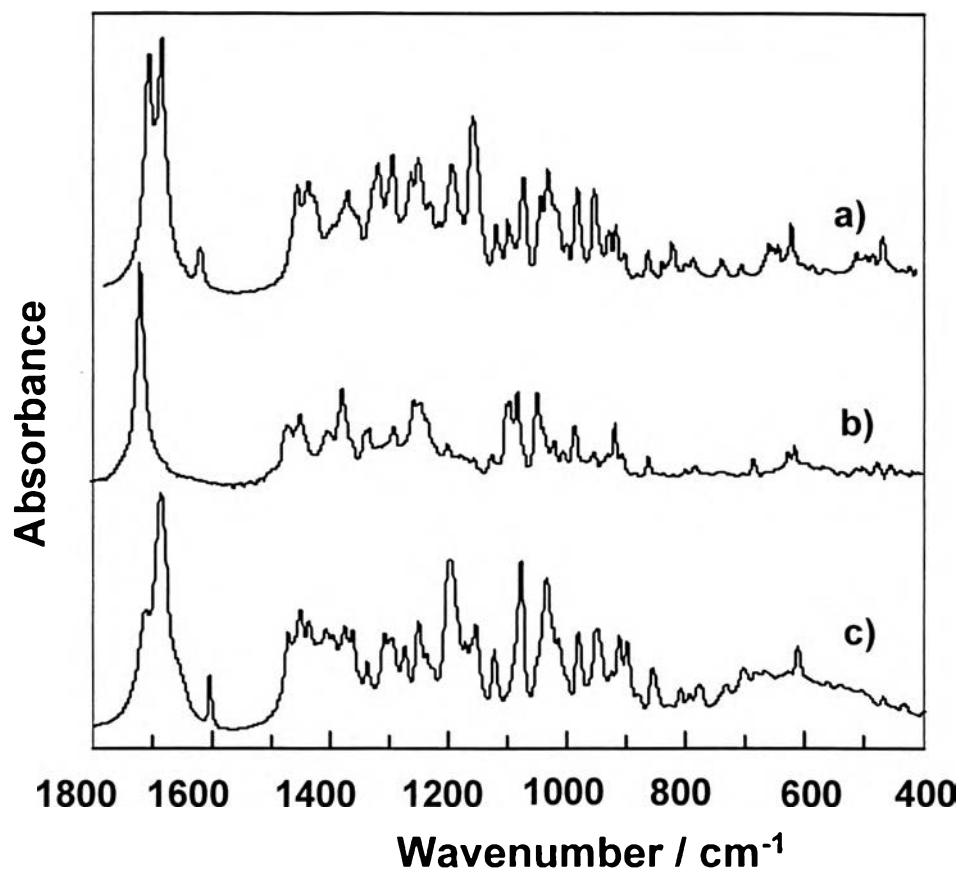
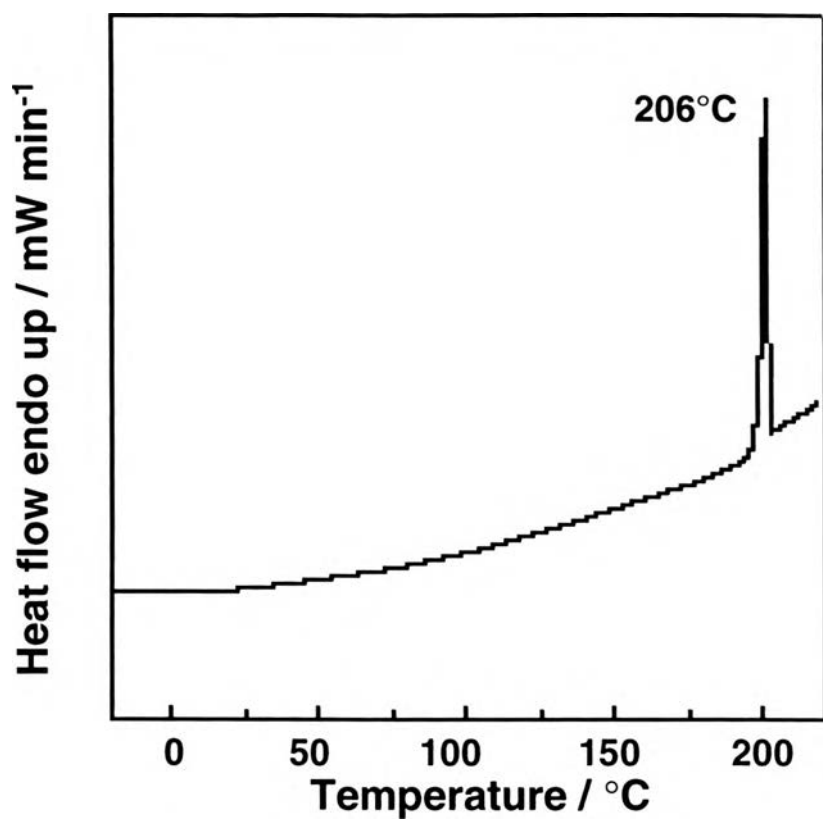**Figure 4.1** FT-IR spectra of (a) CA-MMA; (b) CA-MMAGF; and (c) CA-VCM.

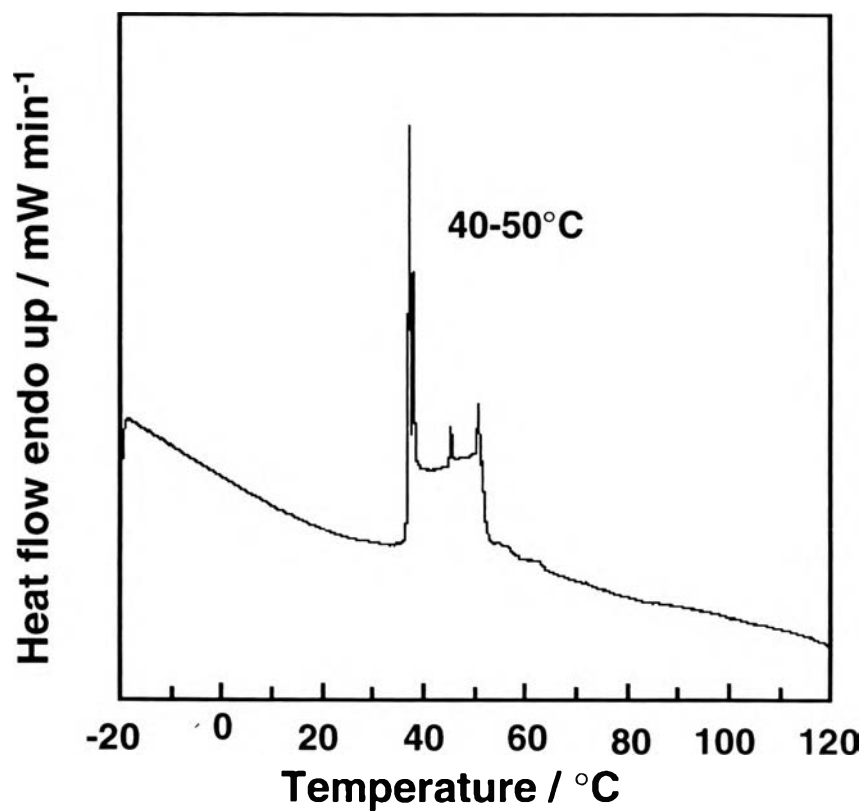**Figure 4.2a** DSC thermogram of CA guest free.

Figure 4.2b DSC thermogram of CA-VCM.

4.2 Inclusion polymerization of CA-VCM

For inclusion polymerization, there are factors to be concerned, i.e., the amount of γ-ray, postpolymerization time, and the effect of host channel.

4.2.1 Effect of γ-ray on the inclusion polymerization of CA-VCM

The amount of γ-ray initiating inclusion polymerization of VCM was studied. In the present work, the dose of γ-ray was varied for 10, 20, 30, and 40 kGy. The γ-ray radiation effects on the molecular weight and the polymer yield percentage, as shown in Figure 4.5. When the dose was increased, the molecular weight decreased. This can be explained that, the increase of dose induced more radical species in the system while the polymerization step leads to the short polymer chain. In another way, the PVC yield (g of PVC/mol of CA), (Figure 4.5), increased with an increase of dose, and decreased significantly at dose 40 kGy. It should be noted that γ-ray radiation induced the polymerization among radical species as well as chain degradation. At dose 10-30 kGy, the polymerization might be more significant than chain degradation. As a result, PVC yield increased gradually. However, for the high dose at 40 kGy, the process of chain degradation came to play the role. In the present case, there were short polymer chains as well as the degraded polymer chains. In the polymer collection procedures, these polymer chains would be dissolved in the solvent and excluded from the system. As a result, the collected amount of PVC obtained from high dose was less than that of PVC obtained from low dose. Thus, the apparent polymer yield was low.
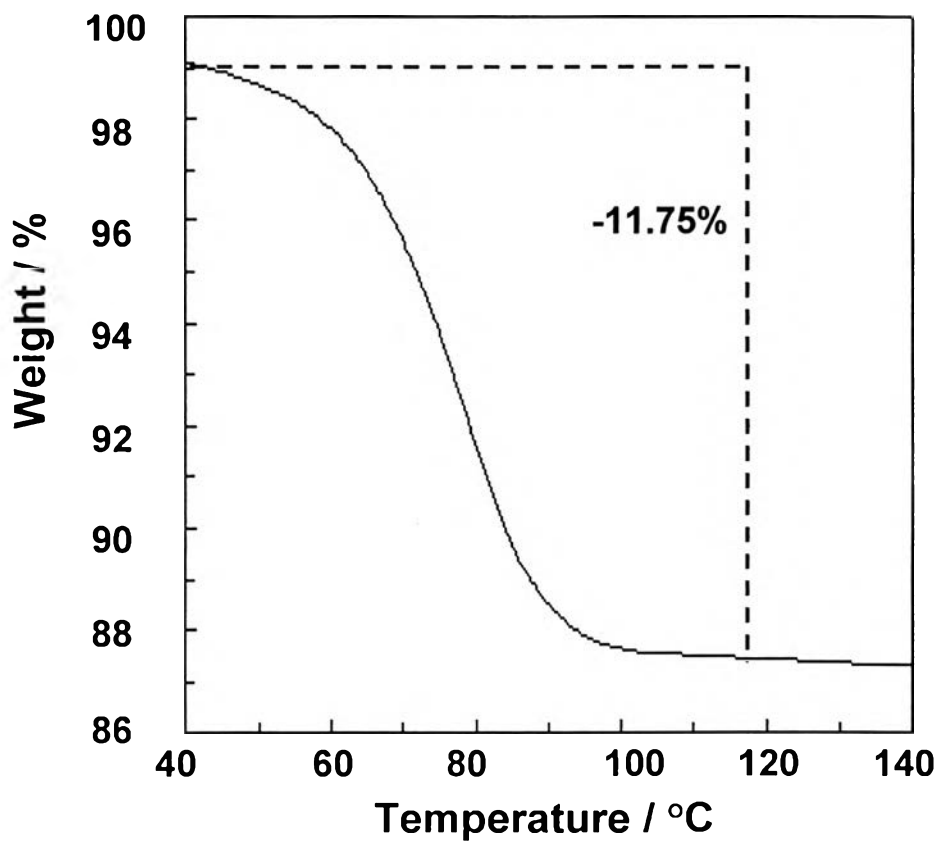
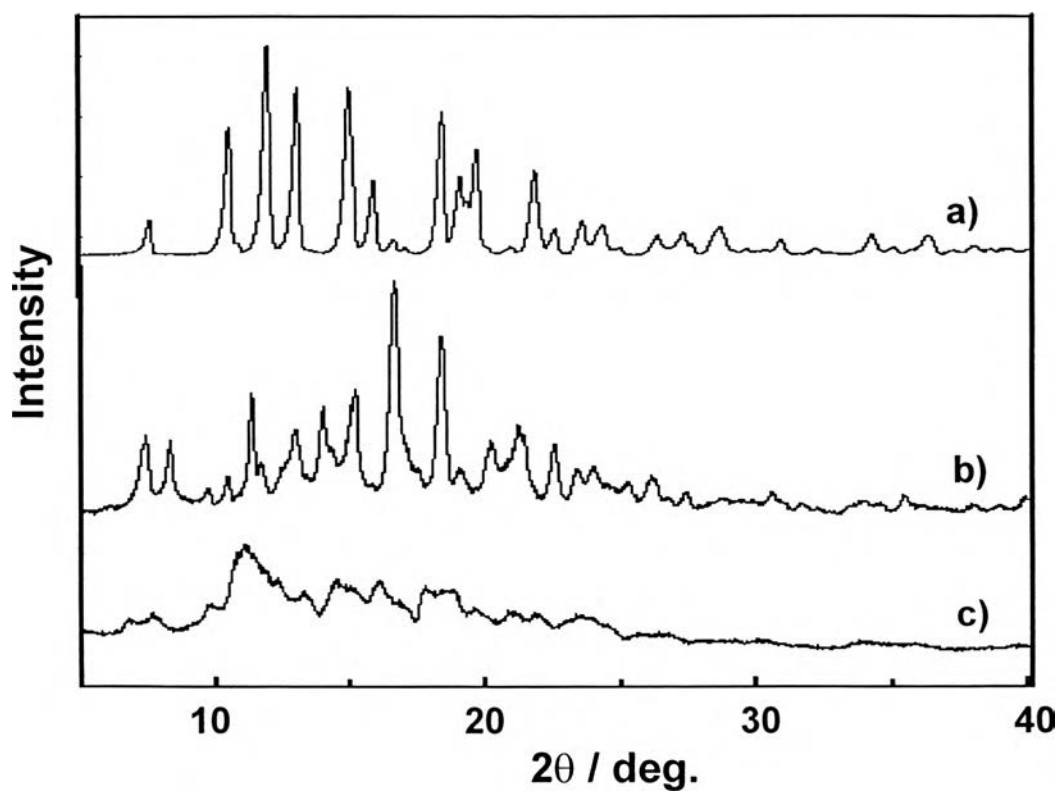**Figure 4.3** TGA thermogram of CA-VCM.

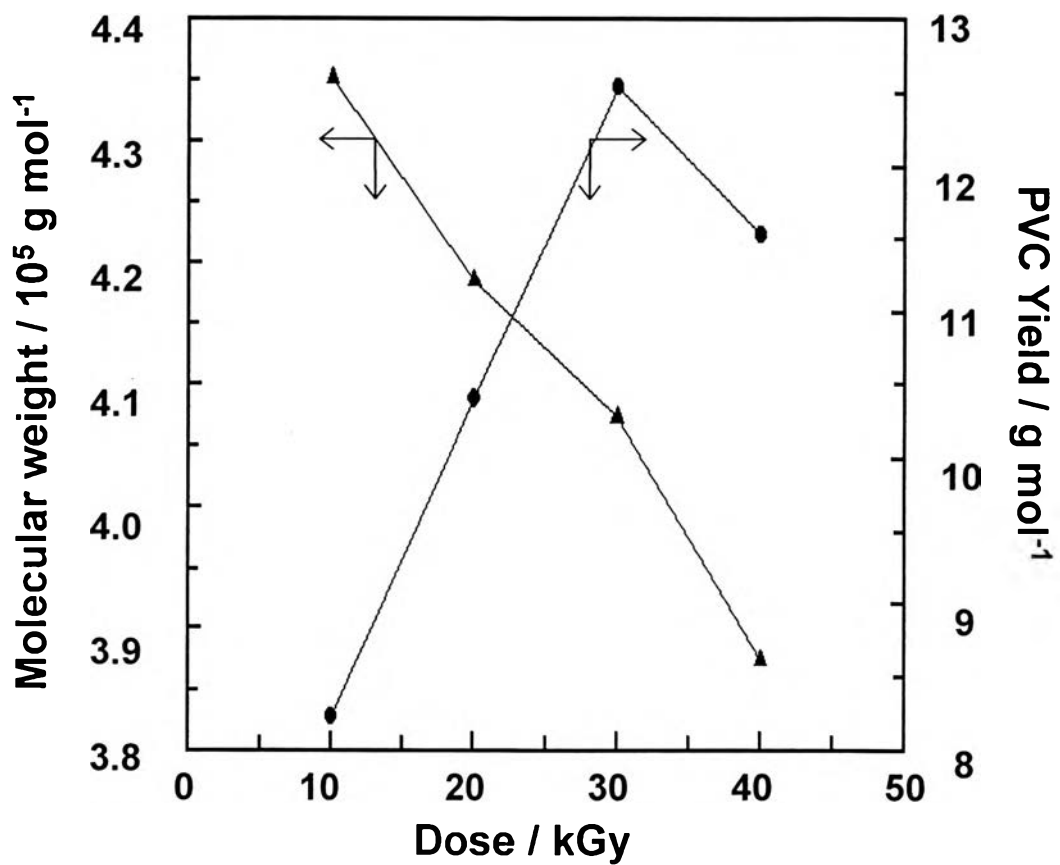**Figure 4.4** XRD patterns of (a) CA-guest free; (b) CA after VCM insertion for 7 and (c) 2 days.

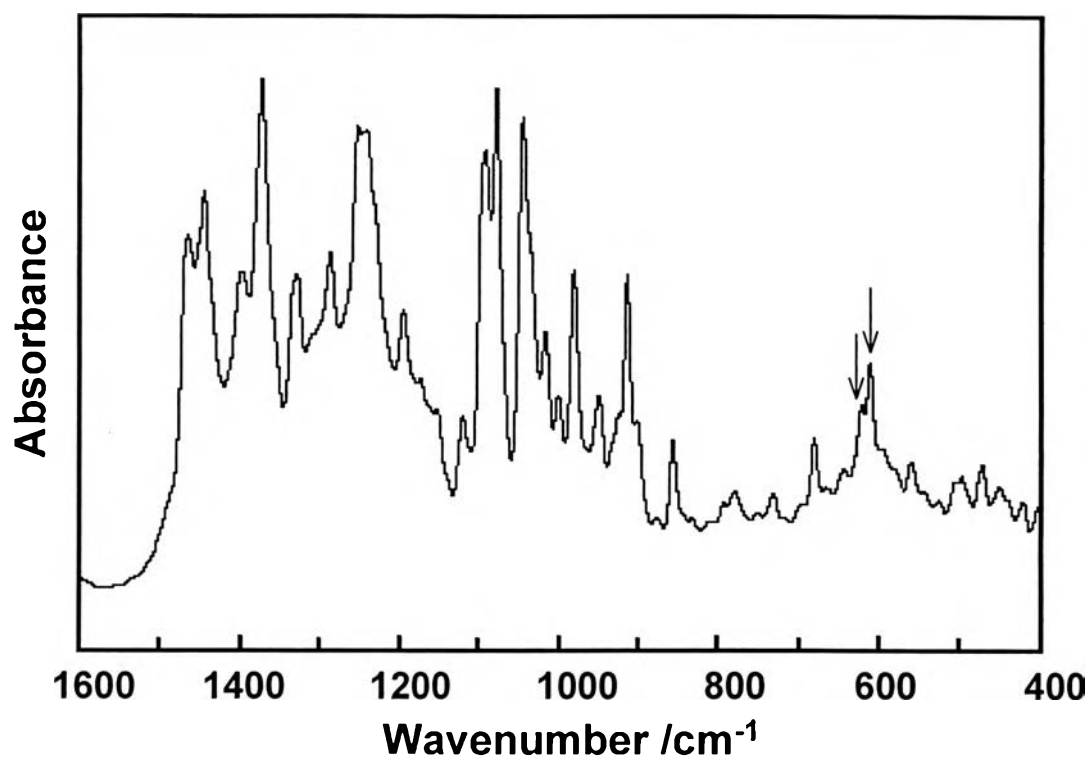**Figure 4.5** Molecular weight and PVC yield as a function of dose.

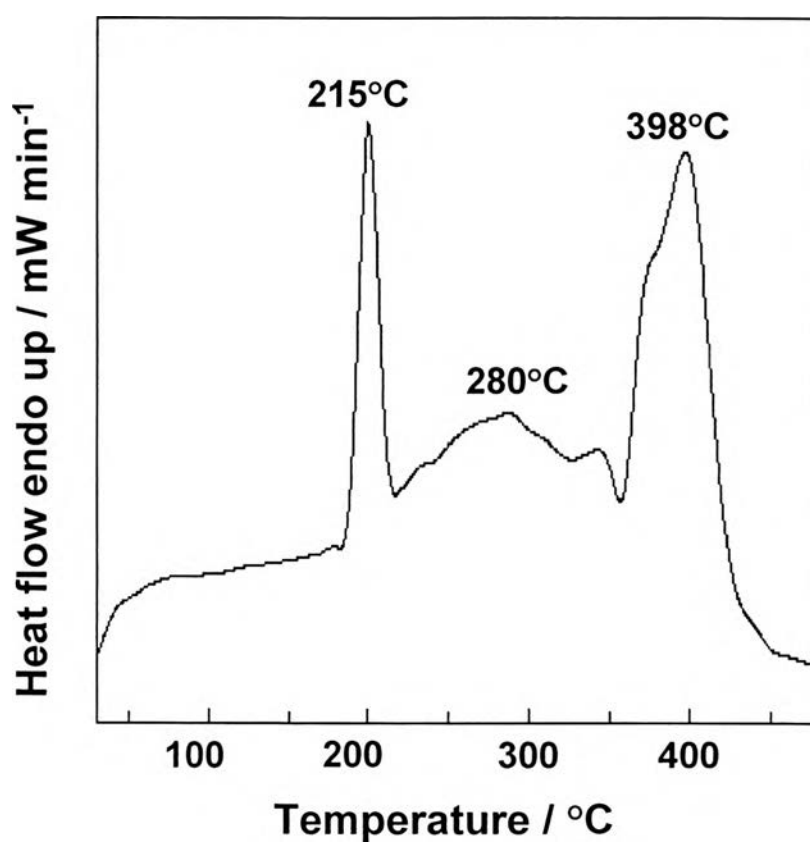**Figure 4.6** FT-IR spectrum of CA-VCM after radiation.

Figure 4.7 DSC thermogram of CA-VCM after radiation.

4.2.2 Effect of postpolymerization time on the inclusion polymerization of CA-VCM

After γ-ray radiation, the postpolymerization was left at -15°C, for 7, 14, 40 days. The obtained PVC in terms of molecular weight, molecular weight distribution (MWD) and polymer yield percentage were studied. As shown in Table 4.1, molecular weight shows only small increase. This might be due to the fact that the host cavity limits the movement of monomer radical to go along the channel after a certain polymer chain was produced. However, the PVC yield increased as the postpolymerization time increased. Table 4.1 shows the decrease in molecular weight distribution of the obtained PVC when postpolymerization time was increased to 40 days. This might be that the result of the longer time in postpolymerization provided effective radical polymerization to obtain polymer at a similar chain length.

Table 4.1 Molecular weight, PVC yield and MWD as a function of postpolymerization time

Time (days)	%Yield	MW	MWD
7	3.40	243 741	1.41
14	4.57	241 266	1.37
40	5.29	258 626	1.34

4.2.3 Inclusion compound of CA-VCM after γ-ray radiation

In order to clarify the inclusion polymerization of VCM occurring in CA channel, it is our interest to study CA-VCM adducts before and after radiation. Here, CA-VCM host guest compound was expected to change to CA-PVC after radiation.

The adduct after radiation was used directly as it was to confirm inclusion polymerization. As shown in Figure 4.6, the FT-IR of the obtained adduct demonstrated the peaks at 611, 614, and 693 cm^{-1} which assigned to

the vibration mode of C-Cl stretching of PVC. DSC thermogram (Figure 4.7) of CA-PVC shows three endothermic peaks at 215, 280, and 398°C. The peak at 215 and 398°C refer to the melting point of CA and decomposition, respectively. Thermal analysis of commercial PVC was operated to find the degradation belonging to HCl elimination at 280°C. Therefore the peak at 280°C was due to the degradation of hydrochloric acid from PVC in CA channel. This small peak at 280°C supported that PVC was generated in CA host channel, or in another words, insertion of CA-VCM is successful.

XRD was used to confirme structural changing of CA-VCM after radiation (Figure 4.8). It is known that when the inclusion polymerization occurs, the crystal pattern will be changed. The XRD pattern of CA-VCM after radiation shows 2θ at 6.8, 9.8, 11.1, 12.3, 14.3, 15.2, 17.7, and 18.9 degrees which are similar to the peaks of CA immersed in VCM for 2 days but different from guest free CA as compared with Figure 4.4. XRD pattern implies the monomer insertion in CA channel.

4.2.4 Polymerization of VCM in CA channel and on silica surface

Concerning on the structure of CA-VCM, it can be thought that VCM can be changed to polymer either on the surface (physisorption) or in the channel. Thus, silica gel was applied as a substrate for physisorption of VCM. The γ-radiation of silica-VCM was studied as the case of CA-VCM.

The molecular weight obtained from inclusion PVC shows 2 peaks of inclusion PVC at 4 362 and 407 409 (Figure 4.9(a)). However, irradiated silica-VCM gives only 1 peak at 4 539 (Figure 4.9(b)). The low molecular weight could be claimed to the polymerization occurring on the surface of silica or CA crystal. In another words, the high molecular weight reflected the PVC obtained via a continuous polymerization condition. This condition should come from the specific inclusion polymerization in CA host channel, i.e., the high molecular weight PVC occurred in the channel where the long live radical prevented termination.
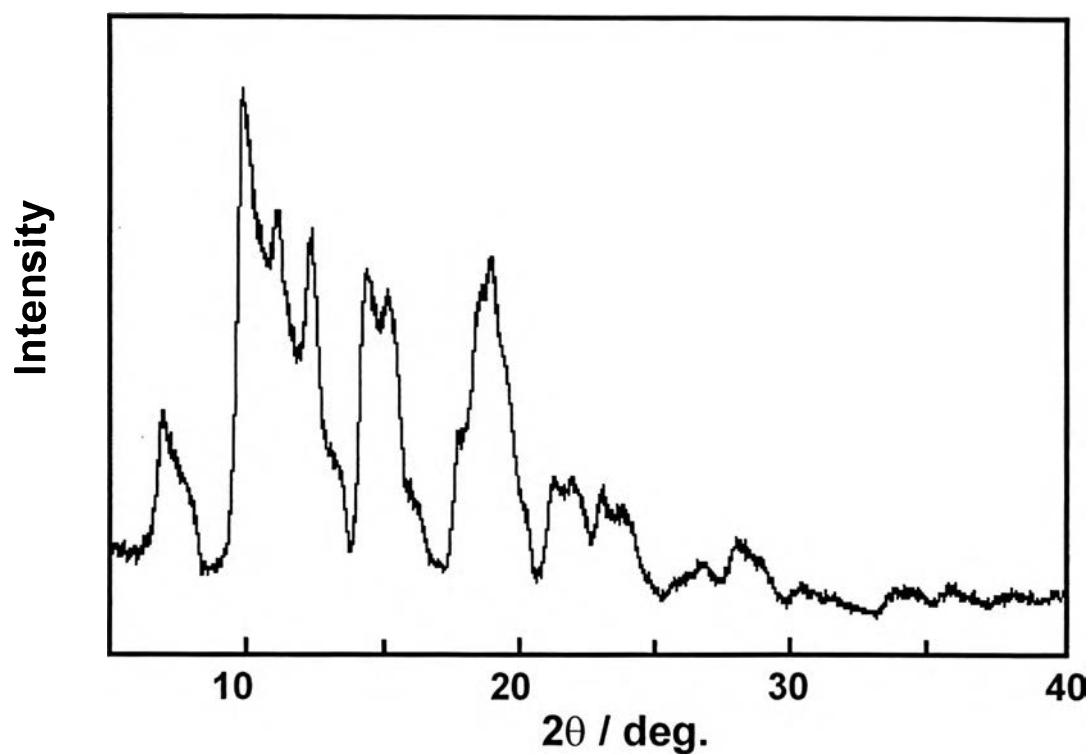
Figure 4.8 XRD pattern of CA-VCM after radiation.
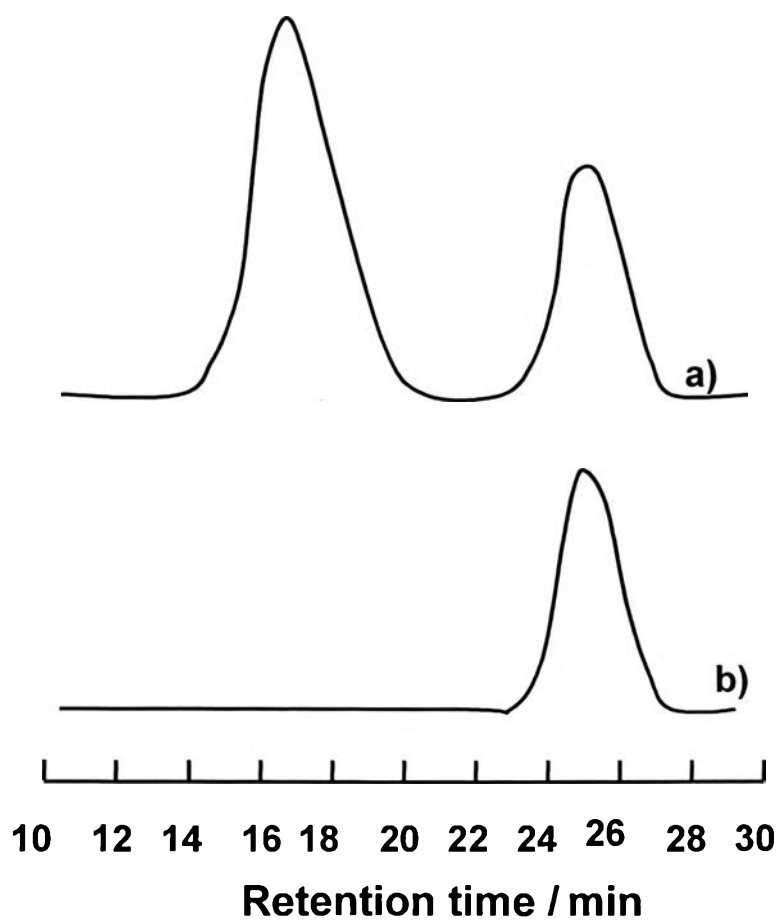

Figure 4.9 GPC chromatograms of (a) PVC-inclusion; (b) PVC-silica.

4.3   Structural analysis of the obtained PVC

Minagawa *et al.* (1999) reported that the inclusion PVC obtained from the urea channel showed the highly stereoregular PVC by solid-state NMR. Here, the stereoregularity of the obtained PVC was evaluated. Figure 4.10 shows FTIR spectra of the obtained PVC comparing to that of the commercial PVC and PVC-silica. In either case, the resulting polymer can be concluded as poly(vinyl chloride). The stereoregularity peaks are referred to 1 428 and 1 434 cm^{-1} for the C-H stretching of syndiotactic, and isotactic methylene species, respectively, as reported by Germarn *et al.* (1963), while 640 and   690 cm^{-1} for C-Cl stretching of isotactic and syndiotactic ones, respectively, as reported by Krimm *et al.* (1958). Quantitative FTIR was used to identify the tacticity of PVC by using the ratio of these characteristic peaks.

Figure 4.11 shows the percentage of syndiotactic and isotactic determined from methylene stretching peak at 2 910 cm^{-1} as an internal standard. Although the C-Cl and C-H stretching peaks gave different tacticity ratio, it can be seen that in either case, the syndiotacticity of silica-VCM and CA-VCM are higher than isotacticity. In the case of silica-VCM, the polymerization was controlled by the low temperature and the propagation occurred on the surface of silica. As a result, the syndiotactic might be obtained. However, in the case of CA-VCM, the polymerization was controlled by the space of the channel which limits the movement of radical species at a certain level. Thus, the obtained PVC might show high syndiotacticity.

The resulting PVC from CA-VCM (Figure 4.12a) was characterized by ^{1}H-NMR and was compared to that of PVC obtained from silica-VCM (Figure 4.12b) and commercial PVC (Figure 4.12c). The peaks from 4 to 5 ppm were assigned to the proton of CHCl. The peaks from 2 to 2.5 ppm represented methylene protons of PVC backbone. A few peaks at 1 and 2.4 ppm were due to the residue of CA, which might be included in the PVC

chain as a terminal group when the radical polymerization occurred. The peaks splitting at 4.5, 4.4, and 4.2 ppm shown separately in Figure 4.13, are the characteristic peaks of syndiotactic, heterotactic, and isotactic, respectively. The ratio of the integrated peaks for syndiotactic, heterotactic and isotactic implied the tacticity of the PVC (Table 4.2). Although the precise crystal structure analysis of CA-VCM is required in order to clarify the factor contributed for tacticity by the radical polymerization in CA channel, we thought that the channel of CA for VCM should provide spaces for VCM to move or rotate along the channel, as a result, the syndiotacticity is achieved at a certain level.

Table 4.2 Percent regularity of each PVC observed by ^{1}H-NMR

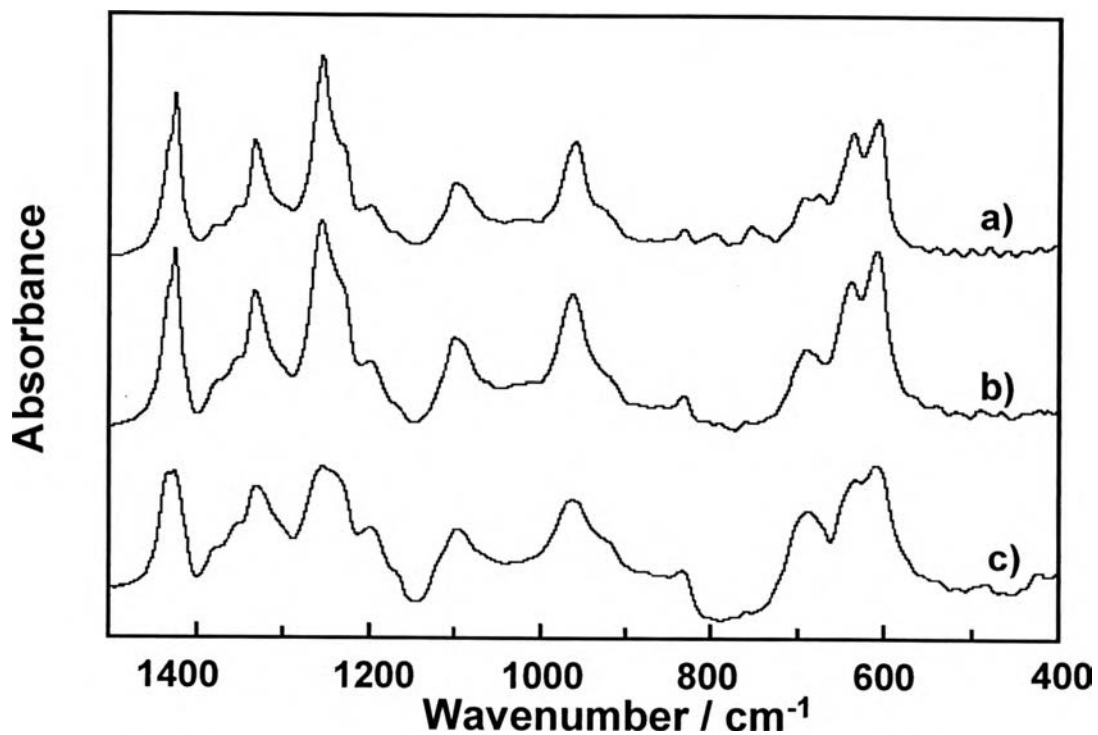| Sample	Isotactic (%)	Heterotactic (%)	Syndiotactic (%)
PVC-inclusion	10.38	42.45	47.71
PVC-silica	11.34	43.3	45.36
PVC-commercial	23.66	48.39	27.96

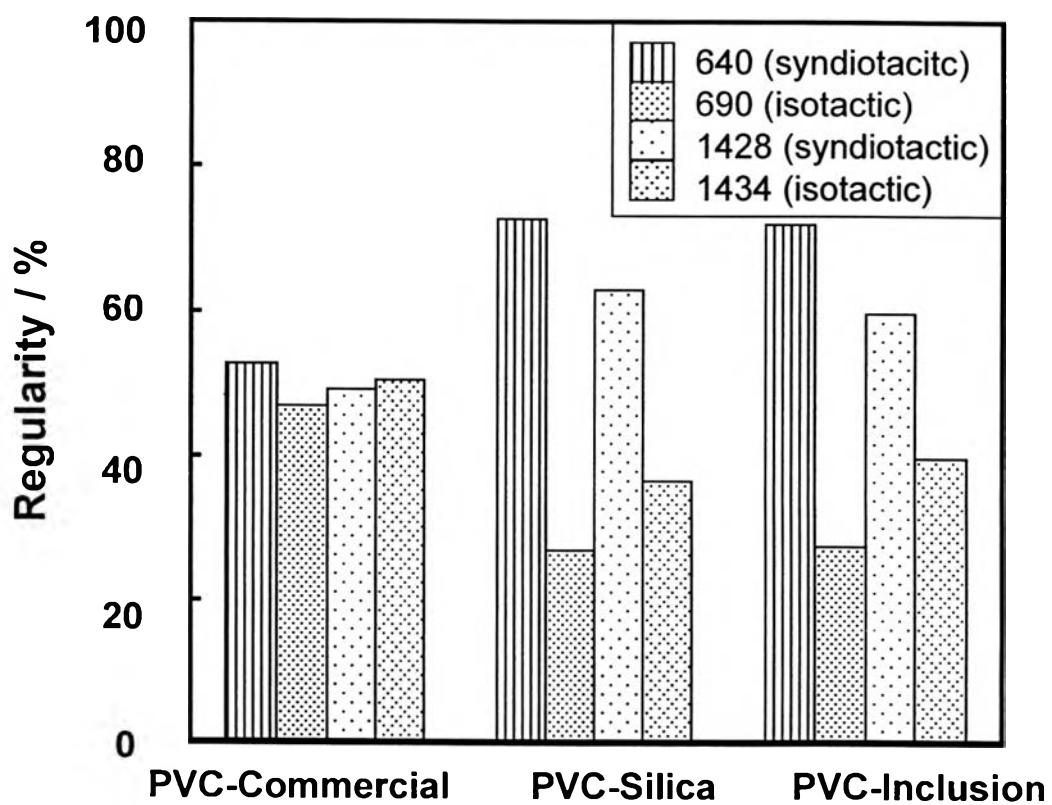**Figure 4.10** FT-IR spectra of (a) PVC-silica; (b) PVC-inclusion; and (c) PVC-commercial.

Figure 4.11 Percent Regularity of PVC-commercial; PVC-silica; and PVC-inclusion from quantitative FT-IR.
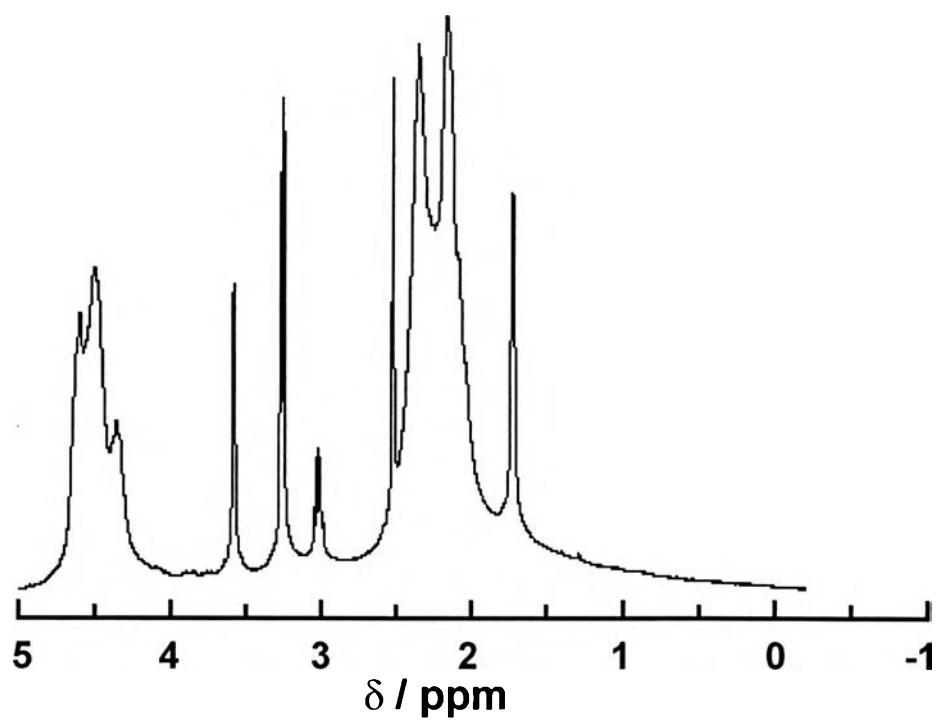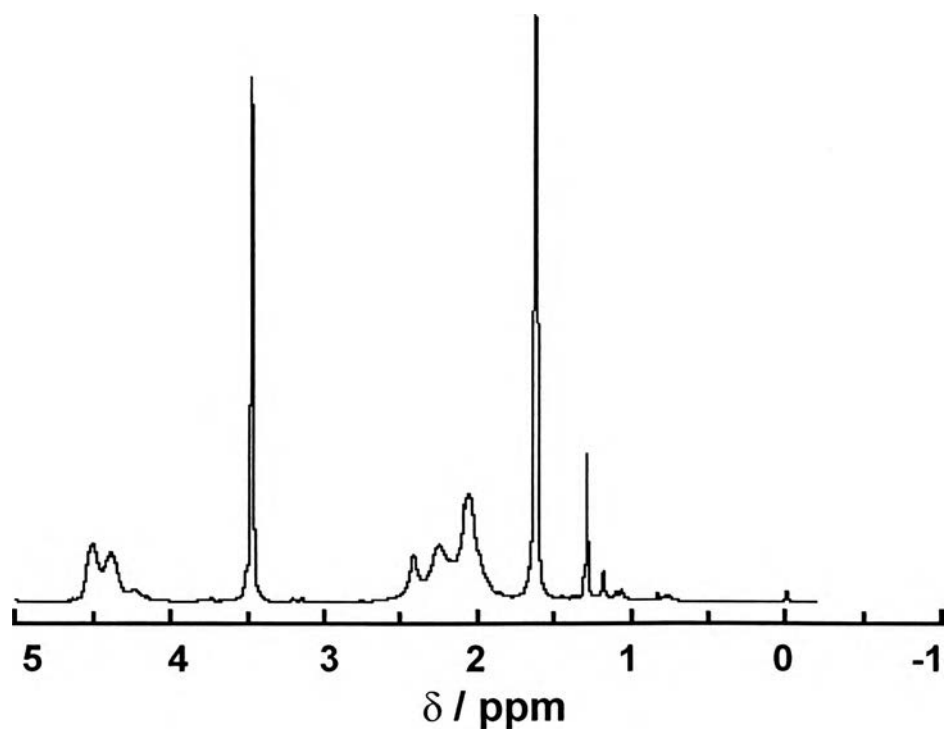
Figure 4.12a ^{1}H-NMR spectrum of commercial PVC.
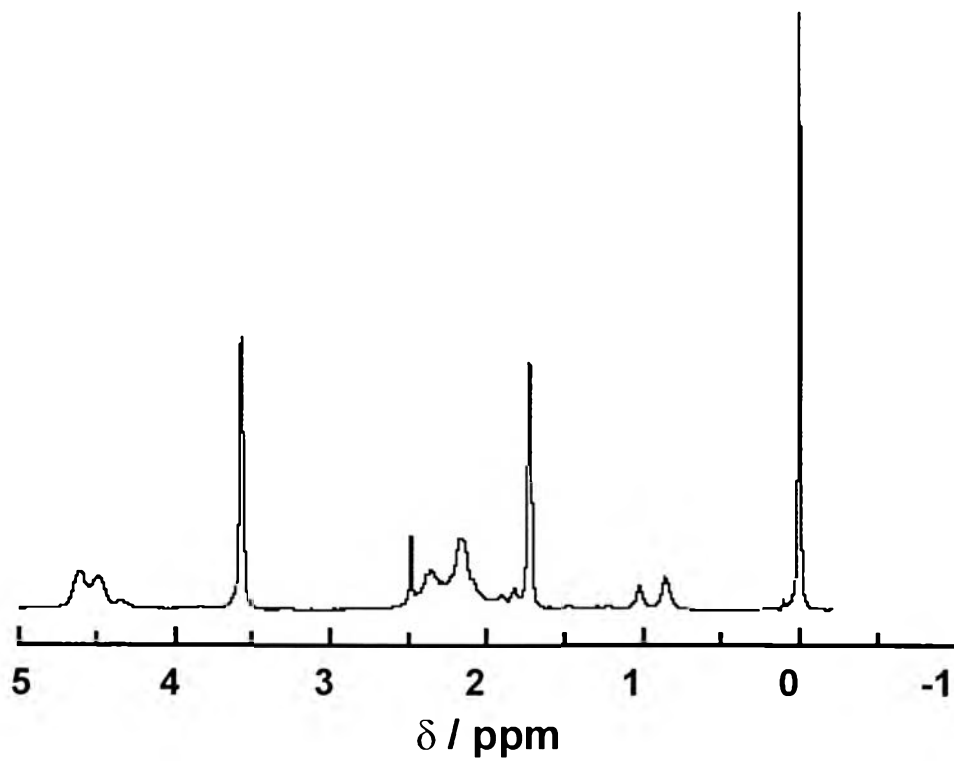

Figure 4.12b ^{1}H-NMR spectrum of PVC-silica.

δ / ppm

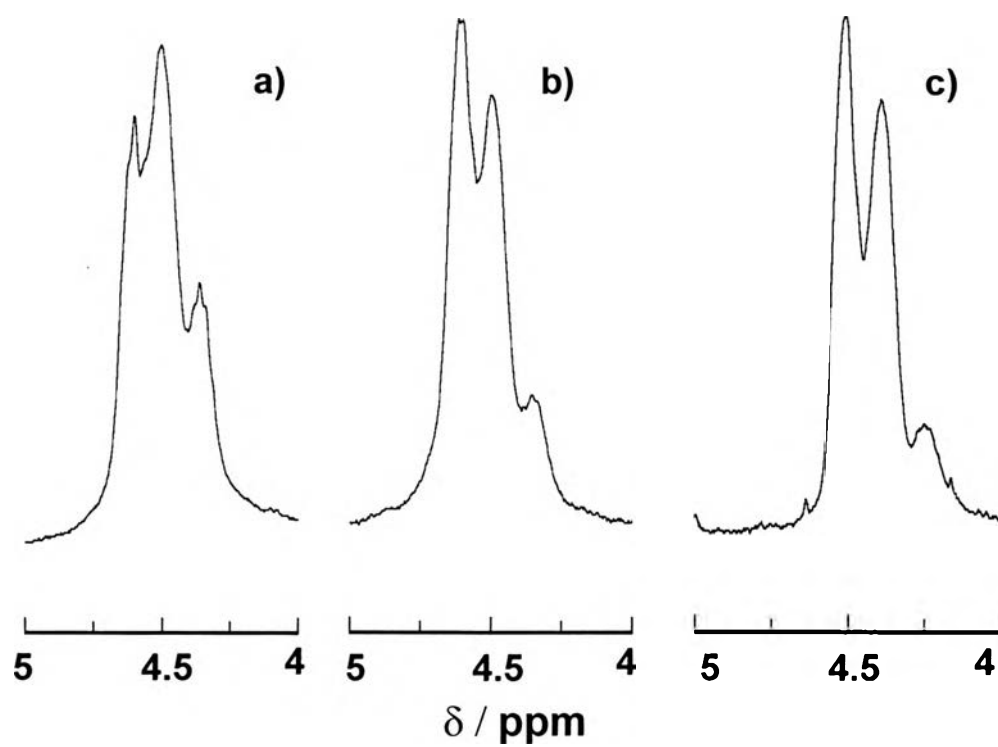**Figure 4.12c** ^{1}H-NMR spectrum of inclusion PVC.

Figure 4.13 ^{1}H-NMR spectra comparing of (a) PVC-commercial; (b) PVC-inclusion; and (c) PVC-silica.